

Analysis of Mutual Acoustic Coupling in CMUT Arrays Using an Accurate Lumped Element Nonlinear Equivalent Circuit Model

H.Kağan Oğuz, Abdullah Atalar, and Hayrettin Köymen

Bilkent University, Electrical and Electronics Engineering Department, Ankara, Turkey

Email: oguz@ee.bilkent.edu.tr



Abstract—We use an accurate nonlinear equivalent circuit model to analyze CMUT arrays with multiple cells, where every cell in the array is coupled to other cells at their acoustic terminals through a mutual radiation impedance matrix. We get results comparable to finite element analysis accuracy. Hence, the analysis of a large array becomes a circuit theory problem and can be scrutinized with circuit simulators. We study the mutual acoustic interactions that arise through the immersion medium due to the influence of the generated pressure field by each cell on the others. We compare the performance of different 1D cMUT arrays, where each element is half-wavelength wide and 10 and 20 wavelengths long at the resonance frequency of a single cell.

I. INTRODUCTION

Capacitive micromachined ultrasonic transducers (CMUTs) are usually made up of large arrays of closely packed cells, expecting to radiate powerful, broadband and beam-formed acoustic signals. Surface micromachining technology enables batch fabrication of large CMUT arrays, which resolves cost issues and many physical limitations. Depending on the precision of the process, designers might consider a great number of different array configurations. However, the lack of appropriate design tools prevents an optimization of array performance. Finite element method (FEM) predictions are accurate for small arrays. But, in arrays with large number of elements FEM is computationally very cumbersome and often practically impossible. This necessitates some simplifying assumptions to be made on large models, which produce misleading results. FEM can only be used to test a specific design with a limited number of cells.

By using the proposed model, the linear frequency and nonlinear transient responses of arrays consisting of hundreds of CMUT cells can be achieved in a matter of few minutes. We perform several FEM simulations for small arrays and show that the results are very consistent with the ones obtained by the equivalent model.

II. EQUIVALENT CIRCUIT FOR CMUT ARRAYS

A typical cell layout of an hexagonal CMUT array element is shown in Fig. 1, where a is the radius of the membranes and d_{ij} is the center-to-center separation between the cells. It is possible to describe the acoustic force on each particular

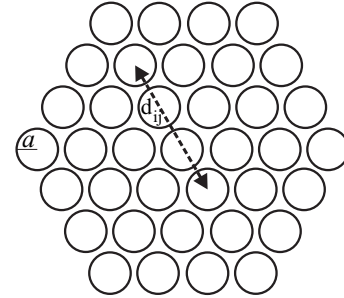


Fig. 1. An hexagonal array of cMUT cells, where the center-to-center displacement between the i^{th} and j^{th} cell is indicated.

cell by the following matrix relationship:

$$\begin{bmatrix} F_1 \\ F_2 \\ \vdots \\ F_N \end{bmatrix} = \begin{bmatrix} Z_{11} & Z_{21} & \cdots & Z_{N1} \\ Z_{21} & Z_{22} & \cdots & Z_{N2} \\ \vdots & \vdots & \ddots & \vdots \\ Z_{N1} & Z_{N2} & \cdots & Z_{NN} \end{bmatrix} \begin{bmatrix} v_1 \\ v_2 \\ \vdots \\ v_N \end{bmatrix}. \quad (1)$$

where F_i and v_i represent the force and the velocity of each cell, respectively. The square matrix, \mathbf{Z} , in Eq. 1, is a complex symmetric impedance matrix. Its diagonal terms are the self radiation impedances, and the off-diagonal terms are the mutual radiation impedances between corresponding two cells.

Once the impedance matrix, \mathbf{Z} , is known, an equivalent circuit model for a CMUT array can be constructed. To do this, we use the single CMUT cell equivalent circuit model [1], given in Fig. 2(a), as the building block of the array and couple them through \mathbf{Z} matrix as depicted in Fig. 2(b).

III. MUTUAL RADIATION IMPEDANCE BETWEEN CMUT CELLS

Analytical expressions for the self and mutual radiation impedances of identical circular clamped edge radiators located on an infinite rigid plane baffle are given by Porter [2]. In his derivations, the reference lumped velocity variable was chosen as the average velocity over the surface of the radiator. For consistency, this variable and the choice of the through variable in the equivalent circuit, v , in Fig. 2(a), must be the same. Nonetheless, any difference can be resolved with a proper scaling factor, as described in [1].

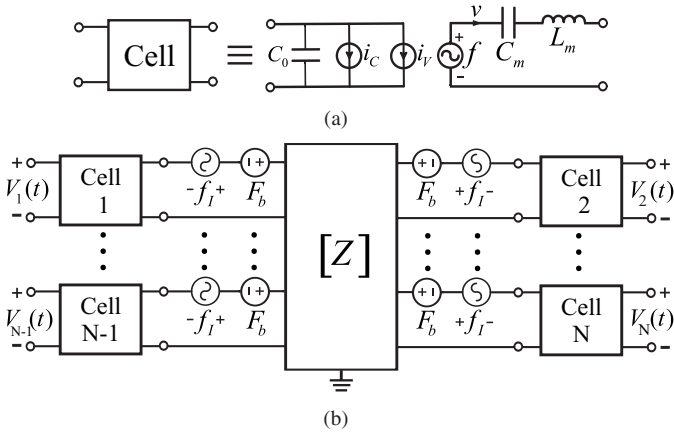


Fig. 2. (a) Equivalent circuit of a single cMUT cell, where (b) N of them are coupled through the \mathbf{Z} matrix. F_b is any static external force (e.g. due to atmospheric pressure). f_I is any dynamic external force (e.g. due to an incident acoustic signal). For an array element, electrical terminals of all cells are connected in parallel: $V_1 = V_2 = \dots = V_N$.

The mutual radiation impedance, Z_{ij} , has a nontrivial expression that is dependent on both ka and kd_{ij} , where k is the wavenumber. It is a slowly decaying function of kd_{ij} , hence ignoring the effects of the distant cells in an array may not be a reasonable assumption. For practical arrays, \mathbf{Z} can readily become a very large matrix and aggravate the performance of circuit simulators. An approximation can be done intuitively, by fitting the following expression to the exact value of Z_{ij} :

$$\frac{Z_{ij}}{\rho c S} \cong A(ka) \frac{\sin(kd_{ij}) + j \cos(kd_{ij})}{kd_{ij}} \quad \text{for } ka < 5.5. \quad (2)$$

where $A(ka)$ is a complex function, which is given in the Appendix.

IV. ACOUSTIC INTERACTIONS IN CLOSELY PACKED CMUT ARRAYS

The single CMUT cell, with the dimensions and material properties given in Table I, resonates at about 3.5 MHz in water, when it is located on an infinite, rigid, plane baffle. In this section, we investigate the effects of mutual interactions when only two, three and four of these cells are closely packed with the numbering given in Fig. 4. The cells are DC biased at 70 percent of their collapse voltage, $V_c = 97V$, and they are electrically driven in parallel with 1 V peak AC voltage.

TABLE I
PROPERTIES OF THE CMUT CELL USED IN THE SIMULATIONS

Dimensions		Material Properties	
Membrane radius	53 μm	Young's modulus	320 GPa
Membrane thickness	4.3 μm	Density	3.27 g/cm^3
Gap height	200 nm	Poisson's ratio	0.263
Insulator thickness	100 nm	Insulator permittivity	4

It is interesting to analyze the cell dynamics for the cell configuration in Fig. 4, because it is the elementary subcomponent of closed packed array elements. In Fig. 3(a), the electrical conductance of the element when only the first two, the first

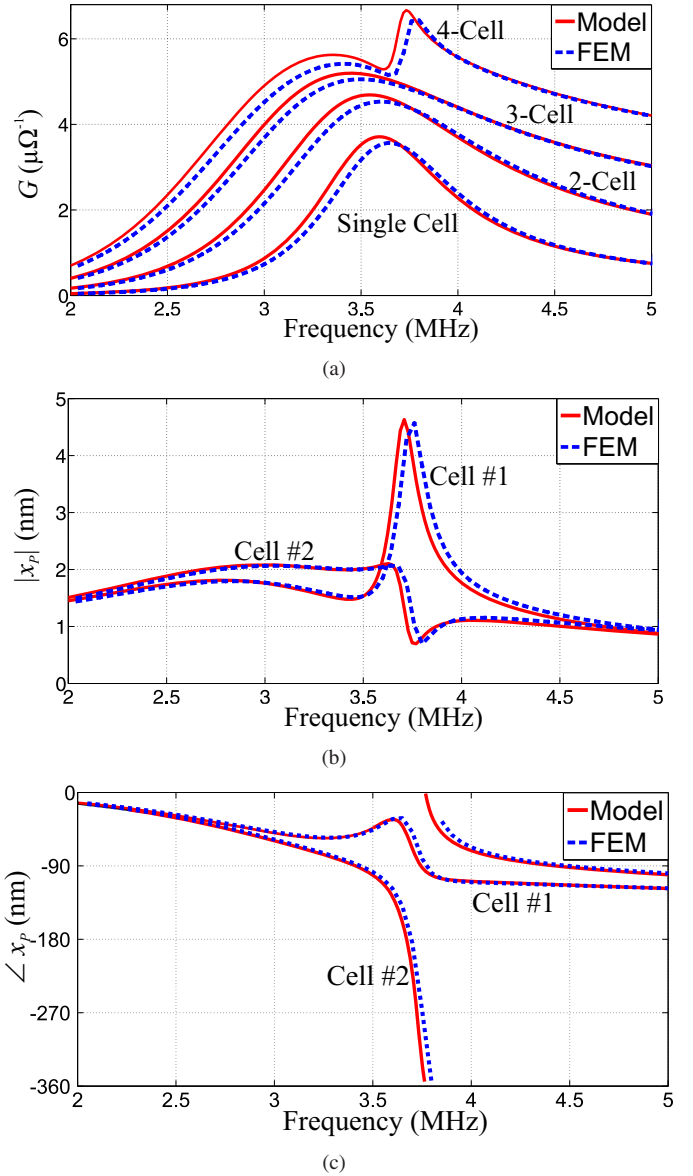


Fig. 3. (a) The electrical conductance of the CMUT element in Fig. 4, when only the first two, the first three and all four cells are present. The cells are driven electrically in parallel and the response is compared with the response of a single cell. When four cells are driven, (b) the magnitude and (c) the phase of the peak displacements of the cell #1 and #2 are shown. The cells are located on an infinite rigid plane baffle and they are immersed in water.

three and all four of the cells are present and driven in parallel. The results are compared with the conductance of the single cell. As the number of cells in the element increase, there is an unproportionate increase in the conductance, which suggests that the radiated power does not increase proportionately, as it would be if the mutual effects were absent.

For the 4-cell case, the results indicate the presence of a spurious resonance. Fig. 3(b) and Fig. 3(c) shows the magnitude and phase of the peak displacement of the cells in the same row. It can be observed that the displacements of these cells differ from each other throughout the frequency band. Notice that the results of the equivalent circuit model and

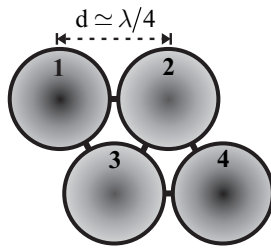


Fig. 4. A configuration of four-cell CMUT array element with reference numbers shown.

FEM match very well. However, the FEM results are obtained in several hours, while it takes just a few seconds to predict the similar results with the equivalent circuit model.

V. CMUT ARRAY ELEMENTS

In general, a CMUT array element may involve 2 to 8 side cells that adds up to $\lambda/2$ or more in the width and can be $L = 10\lambda - 20\lambda$ long, at the center frequency. This means that each array element may contain hundreds of cells, which makes it difficult to simulate the whole array performance. FEM is a widely used and a capable tool, but it is impractical to build and analyze such a large scale model. It is possible to reduce the size of FEM models, when 1-D cMUT array elements are assumed to be infinitely long [3]–[5]. In these reduced models, only the smallest periodic portion of the element is modelled and the solution obtained for this portion is extended to the entire element. However, this approach is very questionable, because the array elements are not infinitely long and the mutual coupling effect does not decay rapidly [6].

A. Frequency Response under linear conditions

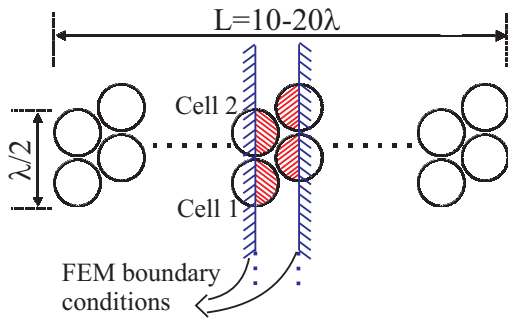
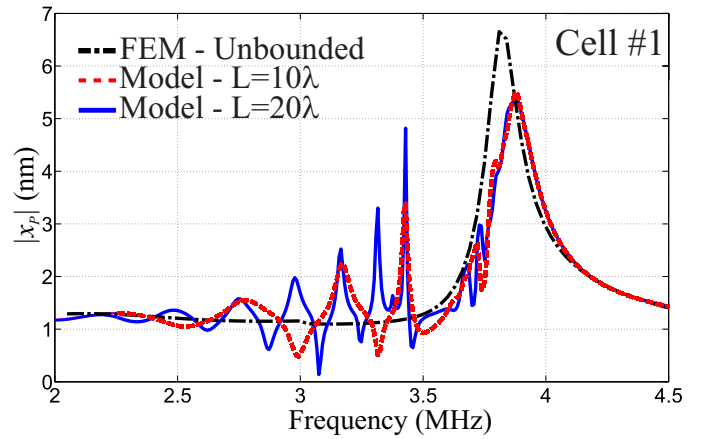
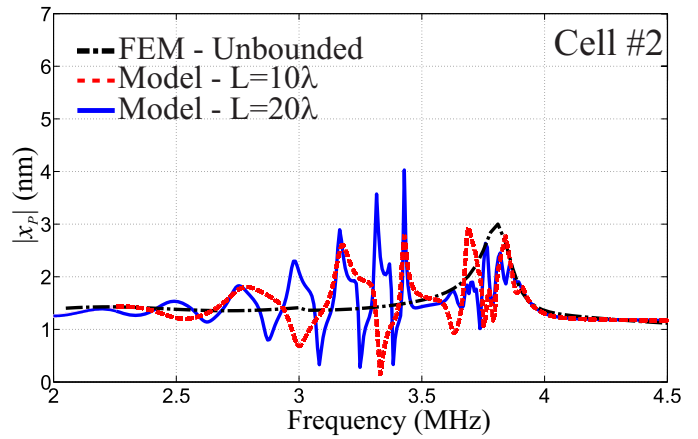


Fig. 5. A 1-D CMUT array element of finite size located on an infinite rigid plane baffle. The rigid boundary conditions applied for the reduced FEM model are depicted assuming an infinitely long array element.

A typical 1-D CMUT array element is shown in Fig. 5. We analyzed this element when its length, L , is 10λ and 20λ at 3.5 MHz in water. The width of the element is $\lambda/2$ with two side by side cells and the edge to edge separation between each pair of cells is $a/10$. The reduced FEM model is also depicted in the figure. Only the dashed cell regions are modelled using periodic boundary conditions. We compared the FEM model results with the equivalent circuit simulations, where we modelled each cell separately and coupled them through



(a)



(b)

Fig. 6. The magnitude of the peak displacement of the two cells that are situated in the middle of the array element given in Fig. 5, when $L = 10\lambda$ and $L = 20\lambda$. The equivalent circuit model predictions include the interactions between all cells in the element. The FEM results are for the reduced model with the infinitely long array element assumption.

the impedance matrix, \mathbf{Z} . The elements have 88 ($L = 10\lambda$) or 176 ($L = 20\lambda$) cells.

FEM model predicts that cells #1 and #4 exhibit the same behavior as do cells #2 and #3. Fig. 6 shows the magnitude of the peak displacements of cells #1 and #2. Both the FEM and the equivalent circuit predict a difference in the response of these two cells. In addition, the circuit model detects many spurious modes, which is due to the finite size of the elements. It is also important to note that the displacements obtained by the circuit model are different for each cell, whereas it is assumed to be periodic in the reduced FEM model. Fig. 7 demonstrates the displacements of the cells for the 10λ long element at 3.26 MHz in water. It can be observed that both the magnitude and the phase of the cells are significantly different. This behavior is an indication of a spurious mode excited around this frequency.

B. Transient Response

The transient response of the 10λ long element is analyzed by using the equivalent circuit model. A voltage pulse of 88V

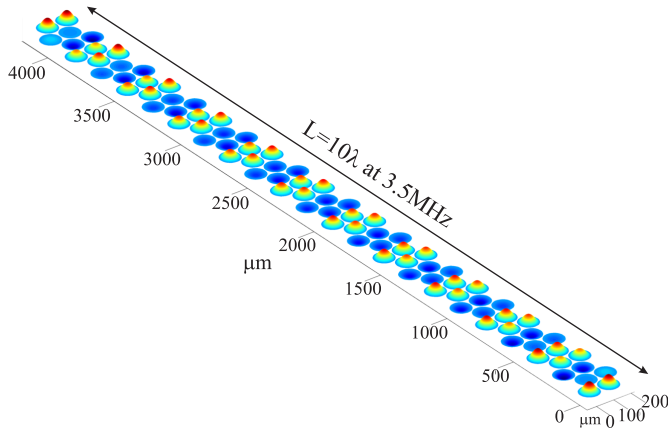
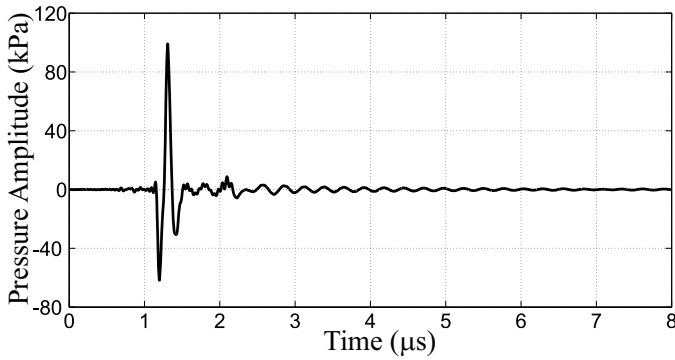
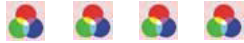
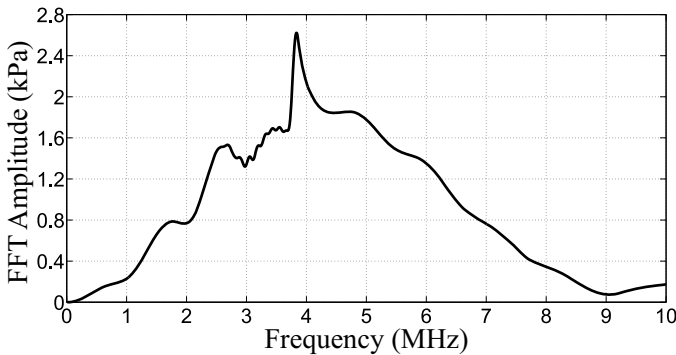


Fig. 7. A 3-D visualization of displacement of cells for the 10λ long CMUT element at 3.26 MHz in water.



(a)



(b)

Fig. 8. (a) The pressure pulse generated with the 10λ long element at 1 mm away from the center of the element and (b) its spectrum.

and $0.1\mu\text{s}$ long with an initial value of 68V is applied to the element. The rise and fall times of the pulse are $0.01\mu\text{s}$. Fig. 8(a) illustrates the time domain pressure pulse generated at 1 mm away from the center of the element. The frequency spectrum of the pressure pulse is given in Fig. 8(b). At nearly $0.85\mu\text{s}$ after the pressure pulse begins, the ringing in the signal is about 20dB below the peak value. Note that the period of the ringing corresponds to 3.9 MHz, which is the frequency of the spurious resonance seen in the spectrum of the signal.

VI. CONCLUSION

The equivalent circuit analysis method for a single CMUT cell is extended to an element containing many CMUT cells. For elements with relatively small number of cells, the results are in very good agreement with FEM results. For elements with large number of cells, the finite element model becomes too large to solve. One has to assume an infinitely long element to generate a reduced FEM model. While the equivalent circuit method predicts the presence of spurious modes, the reduced FEM model does not.

ACKNOWLEDGMENT

This work is supported in part by Turkish Scientific and Research Council (TUBITAK) under project grant 110E216.

APPENDIX

The function $A(ka)$ can be calculated with the 10^{th} order polynomial,

$$A(ka) = \sum_{n=0}^{10} p_n(ka)^n \quad (3)$$

where the real and imaginary parts of its complex coefficients are given in Table II.

TABLE II
POLYNOMIAL COEFFICIENTS OF FUNCTION $A(ka)$

	Real Part	Imaginary Part
p_{10}	-1.74841e-7	-2.07413e-7
p_9	-3.63059e-7	6.41730e-6
p_8	1.00277e-4	-7.76934e-5
p_7	-1.45594e-3	4.43450e-4
p_6	8.20869e-3	-1.06884e-3
p_5	-1.52895e-2	5.31086e-4
p_4	-1.28941e-2	-2.40879e-3
p_3	-2.10234e-2	1.44157e-2
p_2	2.92992e-1	-7.06028e-4
p_1	-2.38707e-3	1.36767e-4
p_0	1.73311e-4	-8.68895e-6

REFERENCES

- [1] H. Koymen, A. Atalar, E. Aydogdu, C. Kocabas, H. K. Oguz, S. Olcum, A. Ozgurluk, and A. Unlugedik, "An improved lumped element nonlinear circuit model for a circular CMUT cell," *IEEE Trans. Ultrason. Ferroelectr. Freq. Control*, vol. 59, no. 8, pp. 1791–99, 2012.
- [2] D. Porter, "Self- and Mutual-Radiation Impedance and Beam Patterns for Flexural Disks in a Rigid Plane," *J. Acoust. Soc. Am.*, vol. 36, no. 6, pp. 1154–1161, 1964.
- [3] S. Ballandras, M. Wilm, W. Daniau, A. Reinhardt, V. Laude, and R. Armati, "Periodic finite element/boundary element modeling of capacitive micromachined ultrasonic transducers," *Journal of Applied Physics*, vol. 97, no. 3, p. 034901, 2005.
- [4] B. Bayram, M. Kupnik, G. G. Yaralioglu, O. Oralkan, A. S. Ergun, D.-S. Lin, S. H. Wong, and B. T. Khuri-Yakub, "Finite element modeling and experimental characterization of crosstalk in 1-D CMUT arrays," *IEEE Trans. Ultrason. Ferroelectr. Freq. Control*, vol. 54, no. 2, pp. 418–30, 2007.
- [5] G. G. Yaralioglu, A. S. Ergun, and B. T. Khuri-Yakub, "Finite-element analysis of capacitive micromachined ultrasonic transducers," *IEEE Trans. Ultrason. Ferroelectr. Freq. Control*, vol. 52, no. 12, pp. 2185–98, 2005.
- [6] A. Caronti, G. Caliano, R. Carotenuto, A. Savoia, M. Pappalardo, E. Cianci, and V. Foglietti, "Capacitive micromachined ultrasonic transducer (CMUT) arrays for medical imaging," *Microelectronics Journal*, vol. 37, no. 8, pp. 770–777, 2006.